JOURNAL OF PROPULSION AND POWER
Vol. 18, No. 2, March–April 2002

Sizing a Slingatron-Based Space Launcher

Mark L. Bundy*
U.S. Army Research Laboratory, Aberdeen Proving Ground, Maryland 21005-5066
Derek A. Tidman†
Advanced Launch Corporation, McLean, Virginia 22101
and
Gene R. Cooper‡
U.S. Army Research Laboratory, Aberdeen Proving Ground, Maryland 21005-5066

A slingatron is the name given to a propellantless mechanical means of launching a projectile. To date, slingatrons are only conceptual in nature, but their potential use as a ground-to-space launch mechanism for unmanned payloads is under investigation. Slingatrons can be configured in a variety of geometries; one form consists of a spiral track (or launch tube) that gyrates at a constant frequency about a set radius. Under proper conditions (design parameters), a projectile entering the spiral at its small radius end will undergo nearly constant tangential acceleration before exiting. The differential equations governing the motion of the projectile within the spiral are highly nonlinear, making the optimum design solution nonintuitive. This paper briefly describes how the slingatron works, then uses the numerical integration procedures within the computer software environment of Simulink® and MATLAB® to search for the minimum-sized slingatron needed to launch a 1000-kg projectile into space.

Nomenclature

A	=	missile cross-sectional area
a	=	geometry factor in determining the distance between loops in an Archimedes spiral
D	=	radius of circular motion
$\boldsymbol{F}_D$	=	force in the radial direction
$\boldsymbol{F}_\perp$	=	force directed normal to the contact surface
$\boldsymbol{F}_\parallel$	=	force directed parallel to, or along, the contact surface
M	=	Mach number
m	=	projectile mass
P	=	average air pressure on front cross section of projectile while inside the slingatron
R	=	slingatron track radius
r	=	radius of gyration for slingatron track
t	=	time
$\boldsymbol{v}$	=	velocity
x	=	horizontal coordinate of projectile in the Earth-fixed coordinate frame
y	=	vertical coordinate of projectile in the Earth-fixed coordinate frame
$\|$	=	absolute value of
β	=	angle describing the spiral geometry
γ	=	either the angle between the normal force and the vector radius for circular motion, or the ratio of specific heats, depending on the context
θ	=	$\psi - \phi$
μ	=	coefficient of friction
ϕ	=	angle of the slingatron track radius relative to the Earth-fixed horizontal axis
ψ	=	angle of the gyration radius relative to the Earth-fixed horizontal axis

Subscripts

0	=	initial value of
$1-n$	=	first through nth value of the subscripted quantity
∞	=	ambient condition
$\parallel$	=	parallel
$\perp$	=	perpendicular

Superscripts

$\cdot$	=	differentiation with respect to time
$'$	=	distinguishes one value of a variable from another

Background

THE cost of launching payloads into space is currently around $10,000 per pound ($22,000 per kg). Although this expense might be acceptable for manned space missions, it can be a curtailing financial burden for other potential enterprises. Less expensive, alternative methods of launching acceleration-insensitive bulk items into space is thus an area of interest. The slingatron is a proposed (propellantless) means of launching objects for such missions.[1–4] This study describes the operational principles of the slingatron and uses Simulink® and MATLAB® to search for the minimum-sized slingatron track needed to propel a 1000-kg projectile into space.

Operation Principles of a Slingatron Launcher

Those who played with a hula hoop as a child and remember how the sound of the ball's speed within the hoop increased with the gyration rate of the hips might recognize the similarity with a projectile in a slingatron. Figures 1–3 show the progression of forces in action in going from uniform circular motion to circular slingatron (or, hula-hoop-type) motion. Specifically, Fig. 1 displays uniform circular motion of a ball of mass m about a circle of radius D with velocity $\boldsymbol{v}$ and centripetal force $\boldsymbol{F}_D$ (all of constant magnitude).

The speed of the ball in Fig. 1 can be increased by orienting the normal force acting on the ball so that it has a tangential as well as a centripetal component. This could be done by envisioning a rotating wedge, as shown in Fig. 2. As the circular speed of the ball increases under the tangential force, so too must the angular velocity of the supporting wedge, as well as the normal force of the wedge on the ball, illustrated in Fig. 2. (Note, if γ in Fig. 2 is positive the speed will increase; if γ is negative, it decreases; and when $\gamma = 0$, the speed stays constant, equivalent to Fig. 1).

Received 14 June 2001; revision received 25 November 2001; accepted for publication 2 December 2001.

*Research Physicist, Weapons and Materials Research Directorate, AMSRL-WM-BC. Senior Member AIAA.
†President, Advanced Launch Corporation. Senior Member AIAA.
‡Research Physicist. Senior Member AIAA.

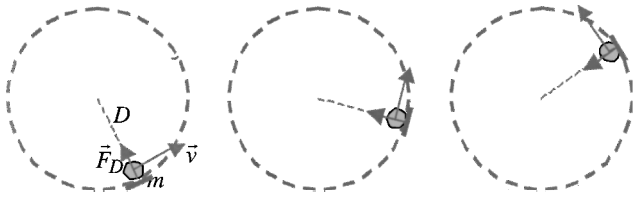

Fig. 1 Uniform circular motion.

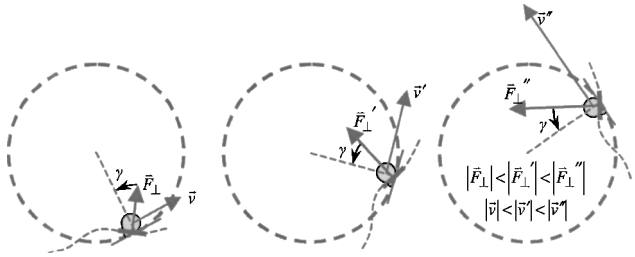

Fig. 2 Nonuniform circular motion created by the tangential force component of a rotating wedge (or wave).

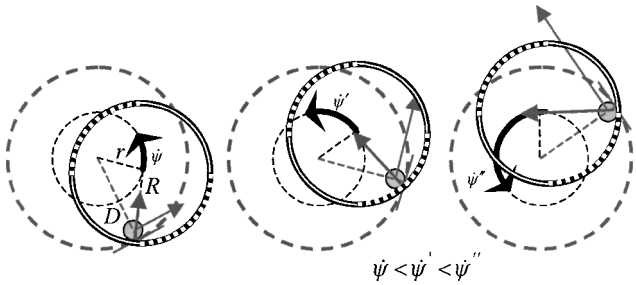

Fig. 3 Nonuniform circular motion created by a gyrating ring.

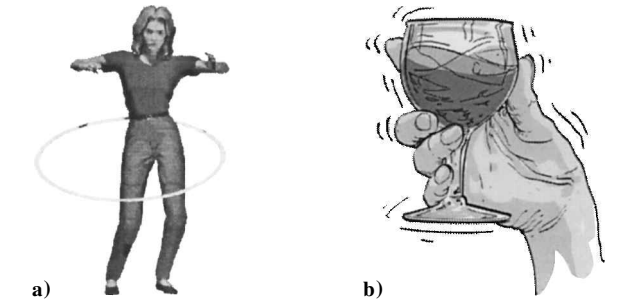

Fig. 4 Slingatron-like motion of a) a hula hoop or b) swirling liquid in a glass.

The effect of the rotating wedge (or wave) on mass m in Fig. 2 can be duplicated by employing a gyrating ring of radius R and therein lies the operational principle of the circular slingatron (or hula hoop), as shown in Fig. 3. As indicted in the illustration, the gyrating ring can provide the same boundary geometry and normal force as the wedge. Like the wedge, the frequency of gyration $\dot{\psi}$ must increase for the ring to maintain its support for and stay in phase with the object.

In addition to the hula hoop, (Fig. 4a), swirling liquid in a cup by moving the hand in a circular pattern (oxidizing wine in glass, for instance) is another practical example of the same effect (Fig. 4b). In this case the wave in the fluid moves up and around the sides of the cup/glass.

Unlike the wedge in Fig. 2, which rotates with the object, the ball in Fig. 3 must execute circular motion within the gyrating ring. Thus, a frictional force of the track on the ball exists. Figure 5 shows the general orientation of the normal and frictional force on the object, as well as specifying a set of reference angles. It can be said that the ring radius R lags the gyration radius r by the phase angle θ $(=\psi - \varphi)$.

Thus far, the discussion has been limited to a circular slingatron track. However, such a configuration poses the practical problem of designing a mechanical gate to release the projectile after it reaches the sought-after Earth-to-space launch velocity. For this reason, an open-ended spiral slingatron is a more feasible projectile-launching track geometry.

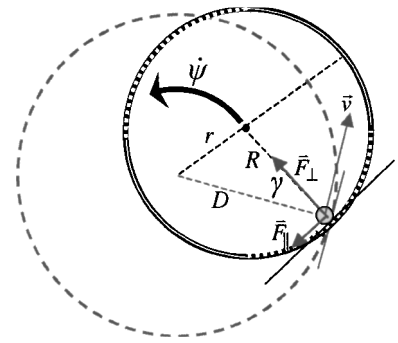

Fig. 5a Normal and frictional force of the ring on the mass.

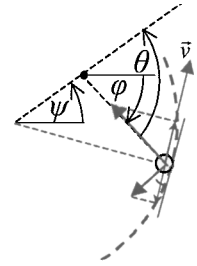

Fig. 5b Normal and frictional force with tangential components of the ring on the mass.

Making the conceptual transition from a circular to a spiral slingatron is facilitated by viewing a spiral that is composed of interconnected semicircular arc lengths (Fig. 6a). At any given location the track is moving within a gyrating circular path, as it was in Fig. 5. Here, however, the radius of the circular arc changes every half-revolution so that an object moving within the launch tube must accelerate in order to complete one revolution in phase with gyrating track (Fig. 6b). Thus, it is conceivable that under the right normal and friction force conditions the object can accelerate, even if the period of gyration is constant.

Equation of Motion for a Slingatron Launcher

The trajectory of the object in Fig. 6 is redrawn in Fig. 7, with the track and the object in motion suppressed to facilitate visualization of the object's velocity, force, and angular orientation. Unlike the gyrating ring of Fig. 5, where the normal force was always directed toward the center of the ring, the direction of the normal force in the gyrating spiral depends on the spiral geometry $R = R(\phi)$, which can also be characterized by the angle β (Fig. 7), defined in Eq. (1). If R does not change with time (or ϕ), the spiral is actually a circle, and $\beta = 0$.

$$\beta = \tan^{-1}\left(\frac{\dot{R}}{R\dot{\phi}}\right) = \tan^{-1}\left(\frac{1}{R}\frac{\mathrm{d}R}{\mathrm{d}\varphi}\right) \tag{1}$$

Aided by Fig. 7, the x and y components of Newton's second law of motion for an object of mass m in the spiral slingatron are

$$\begin{aligned} m\ddot{x} &= |\boldsymbol{F}_\perp|\cos\{\phi-\beta-\pi\} - |\boldsymbol{F}_{||}|\sin\{\phi-\beta-\pi\} \\ &= |\boldsymbol{F}_{||}|\sin\{\phi-\beta\} - |\boldsymbol{F}_\perp|\cos\{\phi-\beta\} \\ m\ddot{y} &= |\boldsymbol{F}_\perp|\sin\{\phi-\beta-\pi\} + |\boldsymbol{F}_{||}|\cos\{\phi-\beta-\pi\} \\ &= -|\boldsymbol{F}_\perp|\sin\{\phi-\beta\} - |\boldsymbol{F}_{||}|\cos\{\phi-\beta\} \end{aligned} \tag{2}$$

In general, the force parallel to the track is caused not only by track friction, but also by air friction/drag; therefore, assume that

$$|\boldsymbol{F}_{||}| = \mu|\boldsymbol{F}_\perp| + PA \tag{3}$$

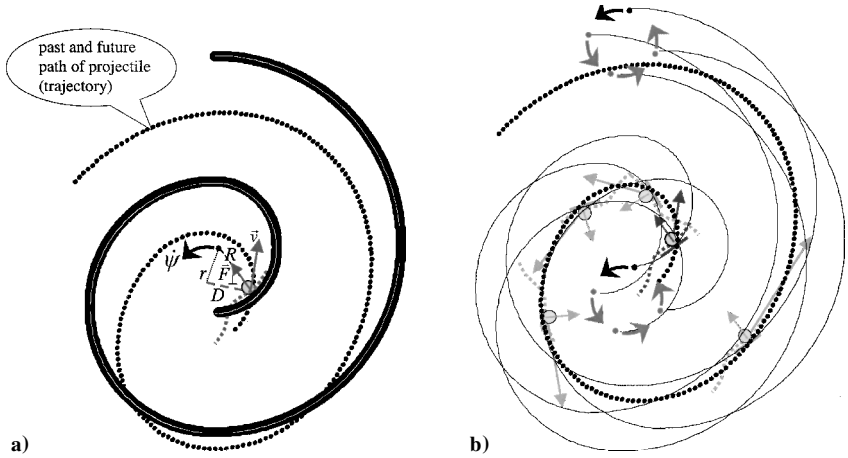

Fig. 6 Spiral slingatron: a) initial and b) first four quarter-cycle gyration conditions.

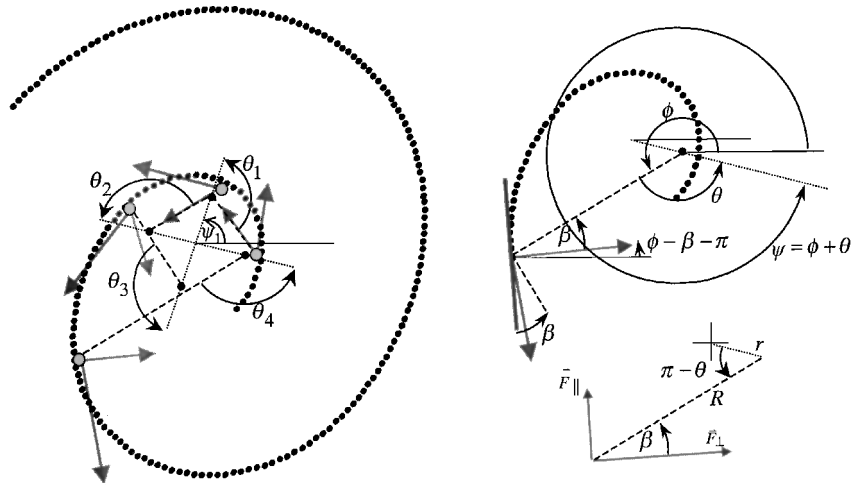

Fig. 7 Kinematics of a spiral slingatron trajectory.

where μ is the coefficient of friction between the circulating mass (ball) and the gyrating track. P is the average frontal air pressure, and A is the object's frontal cross-sectional area. Using Eq. (3) in Eq. (2) yields

$$m\ddot{x}(\sin\{\phi-\beta\}+\mu\cos\{\phi-\beta\})+m\ddot{y}(\mu\sin\{\phi-\beta\}-\cos\{\phi-\beta\})=PA \tag{4}$$

Furthermore, in keeping with the geometry designations of Fig. 7, the x and y components of the objects location can be written as

$$x=r\cos\{\psi\}+R\cos\{\phi\},\qquad y=r\sin\{\psi\}+R\sin\{\phi\} \tag{5}$$

Bearing in mind that r is constant and $R=R(\phi)$, Eq. (4) can be rewritten as [With the exception of the pressure term, Eq. (6) agrees with the equation of projectile motion in a gyrating and evacuated spiral launch tube, as derived by D. A. Tidman in his unpublished notes, dated 11 November 1997.]

$$R\ddot{\phi}[\tan\beta(\mu\cos\beta-\sin\beta)-(\cos\beta+\mu\sin\beta)]+R\dot{\phi}^2\left[\left(\frac{\mathrm{d}\tan\beta}{\mathrm{d}\phi}+\tan^2\beta-1\right)(\mu\cos\beta-\sin\beta)-2\tan\beta(\cos\beta+\mu\sin\beta)\right]+r\dot{\psi}^2[\cos\beta\{\sin(\psi-\phi)-\mu\cos(\psi-\phi)\}+\sin\beta\{\cos(\psi-\phi)+\mu\sin(\psi-\phi)\}]-\frac{PA}{m}=0 \tag{6}$$

In this investigation the only solutions of interest are those for which the gyration rate $\dot{\psi}$ is constant; hence, a $\ddot{\psi}$ term in Eq. (6) is absent. (It is envisioned that size of the spiral slingatron required for Earth-to-space launch will be so massive that it would be difficult to provide such a large structure with any substantial angular acceleration over the short time period that the projectile traverses the launch tube.)

Clearly, this differential equation of motion is nonlinear. A numerical solution is the only one possible. To this end, the numerical integration techniques within MATLAB and Simulink (both marketed by Mathworks, Inc.) are used here to solve the problem. However, before invoking these solution algorithms both μ and P need further clarification. For simplicity the straightforward analytical expression given in Eq. (7) will be used for the average frontal pressure on the object in the slingatron [This expression can be derived from Eq. (3.5), p. 64, of Liepman and Roshko,[5] in the limit of $P/P_\infty \gg 1$ (that is, high object/projectile velocity)].

$$P=P_\infty\gamma(\gamma+1)M^2/2 \tag{7}$$

Here, M is the Mach number of the projectile through the air ahead of it, in which the gas pressure is P_∞, $\gamma=1.4$, and the sound speed is 335 m/s. Under these conditions, it was found that air drag can significantly retard the acceleration of the projectile unless the launch tube is partially evacuated or air is replaced by a lighter gas, such as helium. Because this study is primarily interested in finding the range of possible solutions, it was assumed from the outset that the launch tube could be pumped down to a pressure of $P_\infty=0.01$ atm $=1.01\times10^3$ N/m^2. At this low pressure the drag force has a negligible influence on the solutions of interest here.

The friction coefficient μ is also found to play a significant role in determining the size and speed of the slingatron needed to launch the projectile to an altitude where it could be further carried (for example, tethered) or self-propelled into orbit. The requisite launch velocity for this purpose was assumed here to be 8 km/s. Tidman[6] has obtained experimental data on μ for speeds up to 2 km/s; a curve fit to that data yielded Eq. (8).

$$\mu = \frac{0.12}{1.0 + 2.43 \times 10^{-3}|v|} \tag{8}$$

Assuming Eq. (8) will, through extrapolation, adequately portray the friction coefficient for speeds in the range of 2–8 km/s is troublesome; nevertheless, until a broader range of data is sampled there is little alternative. However, to allay some concern, a test is run for the case where μ is 1.5 times that of Eq. (8); the outcome and implications are discussed.

Solving the Equation of Motion

Spiral Slingatron Parameters

Both the radius of gyration r and the (constant) gyration rate $\dot{\psi}$ are parameters of the problem, as is the mass m and cross-sectional area A of the projectile. Depending on the geometry of the spiral, its description can involve several parameters, for instance, a circle requires one parameter—the radius. For simplicity, a two-parameter Archimedes spiral is assumed here of the form

$$R(\phi) = a\phi + R_0 \tag{9}$$

where a and R_0 are the two parameters. Initial conditions are also needed to specify the starting angles ψ_0 and ϕ_0, as well as $\dot{\phi}_0$. Thus, there are a total of nine parameters that need to be specified in order to unambiguously solve Eq. (6). However, not all of these parameters are varied in this investigation. In particular, ϕ_0 is taken to be 0 rad, thereby defining a reference axis; also, the mass m is taken to be a constant, 1000 kg, as is the projectile's cross-sectional area A, 0.086 m^2 (~2 ft diameter cylinder). Furthermore, it is assumed that $\dot{\phi}_0$ is the same as $\dot{\psi}$ (that is, there is no initial time rate of change in the phase angle θ). Hence, the number of parameters that will be varied in this study is reduced from nine to five.

Solution Results

Although a large range of solutions will ultimately be explored, a small subset is chosen first to demonstrate that some parameters have more influence on the solution than others. With this in mind the initial range of parameters is taken to be

$$\dot{\psi} = \frac{7\pi}{2}, \frac{9\pi}{2}, \frac{11\pi}{2} \text{ rad/s}, \qquad r = 7.5, 9.5, 11.5 \text{ m}$$

$$\dot{\phi}_0 = \dot{\psi}, \qquad R_0 = r + 8, r + 10, r + 12 \text{ m}$$

$$\left.\begin{array}{l} \psi_0 = \dfrac{\pi}{8}, \dfrac{\pi}{10}, \dfrac{\pi}{12} \text{ rad} \\ \phi_0 = 0 \text{ rad} \end{array}\right\} \theta_0 = \frac{\pi}{8}, \frac{\pi}{10}, \frac{\pi}{12} \text{ rad}$$

$$a = 0.175 \times r, 0.225 \times r, 0.275 \times r \text{ m} \tag{10}$$

A command procedure was written whereby the computed Simulink solution of Eq. (6) is obtained for each of the 243 combinations of parameters/initial conditions set out in Eq. (10). A solution for $\phi(t)$ was considered acceptable for the purpose of launching a projectile into space, if the computed value of the projectile's speed within the spiral track reached 8 km/s at any time. Out of the 243 solutions, only 90 produced a projectile speed of at least 8 km/s. One such solution is shown in Fig. 8.

It appears from Fig. 8 that the solution for the projectile's speed increases in a near-linear fashion, almost independent of the phase angle $\theta = \psi - \phi$, until such a time (~40 s) that the phase angle exceeds some critical value; here ~0.6 π rad (~108 deg), above which it grows rapidly, while the speed declines.

Figure 9 plots the acceleration of the projectile in the tangent and normal directions to the spiral for the solution of Fig. 8. Although it is the nonzero tangential acceleration that gives rise to the speed increase, it can be seen that this component is minor in comparison to the acceleration that the projectile undergoes in the direction normal to the track (for example, ~100g vs ~14,000g at the time the projectile reaches 8 km/s).

The high acceleration of the projectile normal to the track requires a large normal force, creating a substantial wall pressure, as displayed in Fig. 10. An accurate strength-of-design analysis of the slingatron track and ground-support structure needed to sustain the

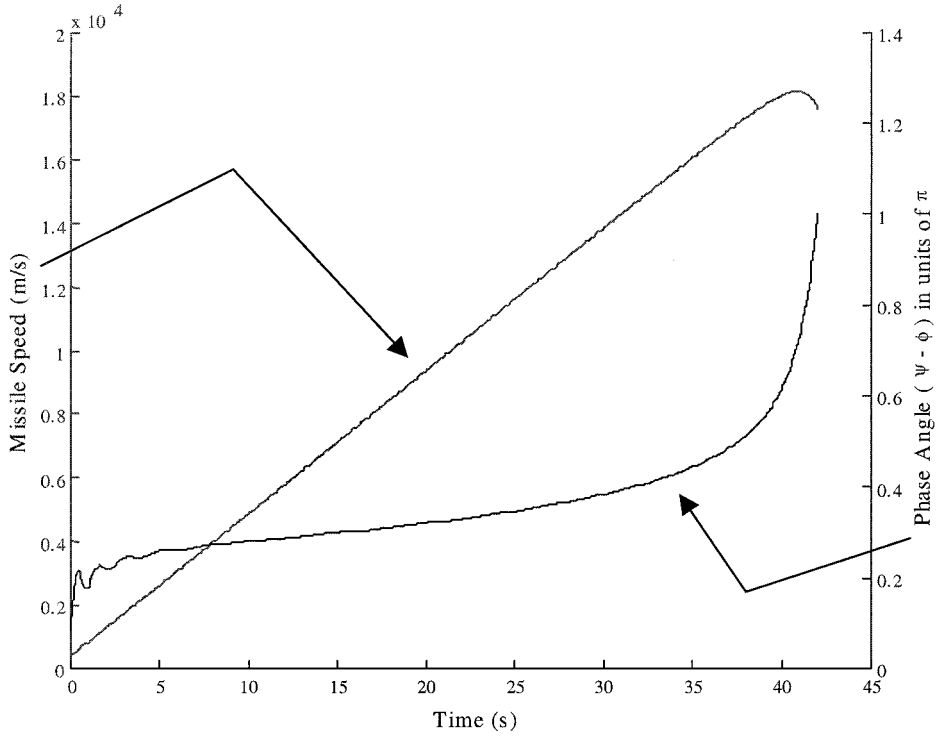

Fig. 8 Simulink solution of Eq. (6) for projectile velocity and phase angle vs time for one of the parameter sets in Eq. (10).

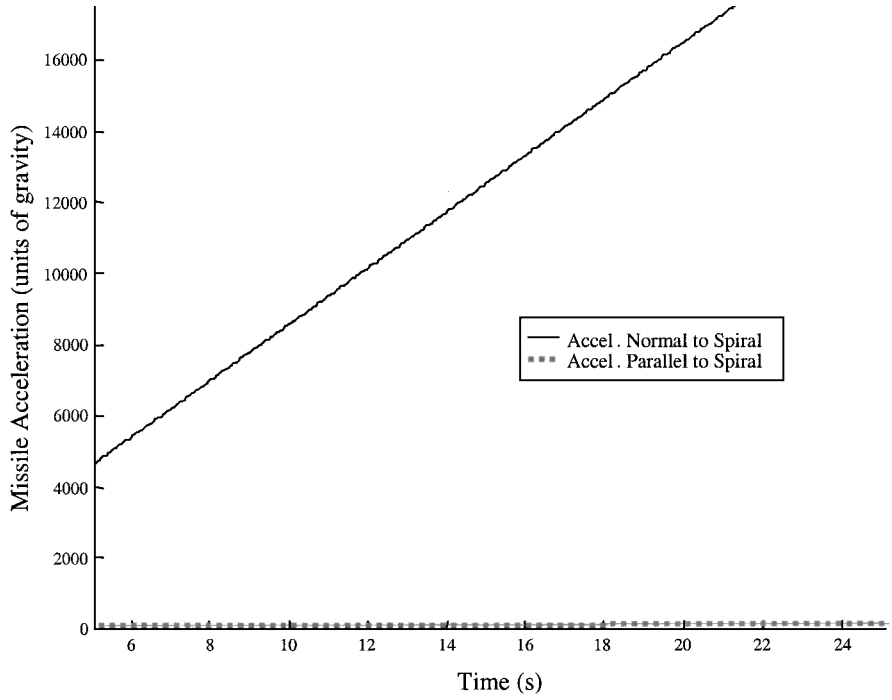

Fig. 9 Acceleration vs time corresponding to the Simulink solution of Fig. 8.

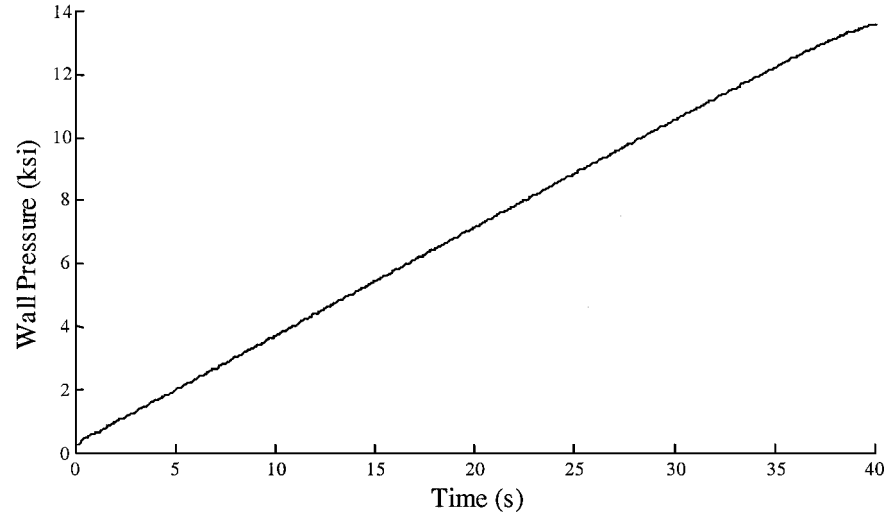

Fig. 10 Projectile-track interface pressure vs time for the solution of Figs. 8 and 9.

pressure loading of Fig. 10 is beyond the scope of the present paper. Nevertheless, an order-of-magnitude approximation for the mass of the spiral track is considered to be of interest. It is for this purpose, and with acknowledged reservation in the accuracy of the estimate, that the following simple rule of thumb (used in the pressure vessel industry) is employed for gauging wall thickness as a function of wall pressure[7]:

$$\text{wall thickness (in.)} = \frac{\text{applied normal pressure (psi)} \times \text{inside cylinder radius (in.)}}{\text{allowable stress (psi)} - 0.6 \times \text{applied normal pressure (psi)}} \tag{11}$$

To compute the total weight of a slingatron track, the total track length needs to be determined. Figure 11 shows the cumulative arc (track) length vs time for the same Simulink solution as that of Figs. 8–10. At 17 s (~8 km/s) the spiral length is ~43 miles. Although not shown here, wall pressure vs track length could also be resolved from the Simulink solution. Similarly, assuming a pipe-like track design made from steel that can safely tolerate a hoop stress of 70 ksi, with inner diameter of 25 in. (corresponding to an A of 0.086 m^2), Eq. (11) can be invoked to provide wall thickness vs arc length. It was thus determined that the 43-mile track would weigh ~17,000,000 lb or 8,500 tons.

Within the 90 parameter sets that yielded successful space-launch solutions, variation in θ_0 did not strongly affect the projectile's speed, its cumulative arc length, nor the wall pressure vs time. A similar result was found to hold for variation in R_0, namely, significant changes in the initial spiral radius produced insignificant change over time in the projectile speed, track length, and wall pressure.

Lastly, as aforementioned, with regards to investigating the influence of the friction coefficient, a single case was run with the expression for μ [Eq. (8)] increased by 50% [that is, the right hand side of Eq. (8) was multiplied by a factor of 1.5]. To compensate for this increase in friction, it was found, for example, that a 35% increase in the radius of gyration r would afford a nearly identical sized spiral to accelerate the projectile to the requisite 8 km/s. The importance of this finding is not in the specifics of which parameters

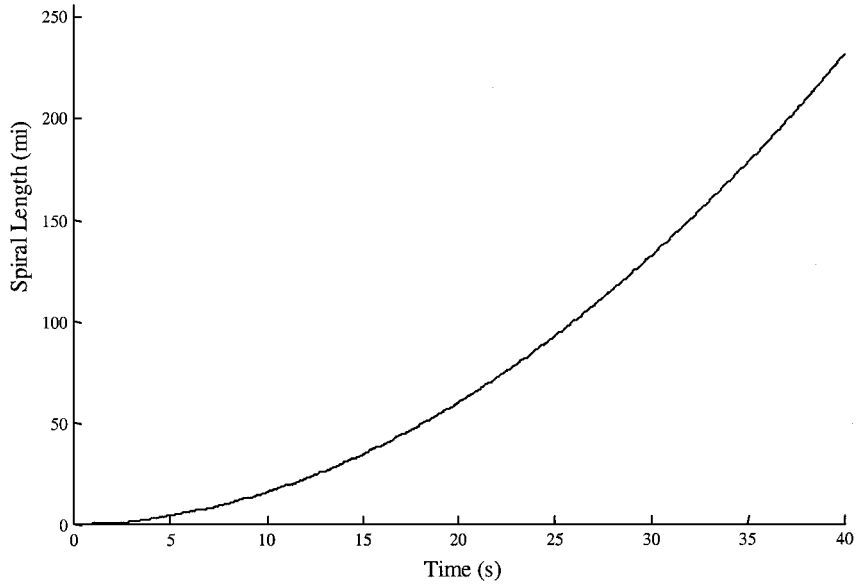

Fig. 11 Track length vs time corresponding to the solution of Figs. 8–10.

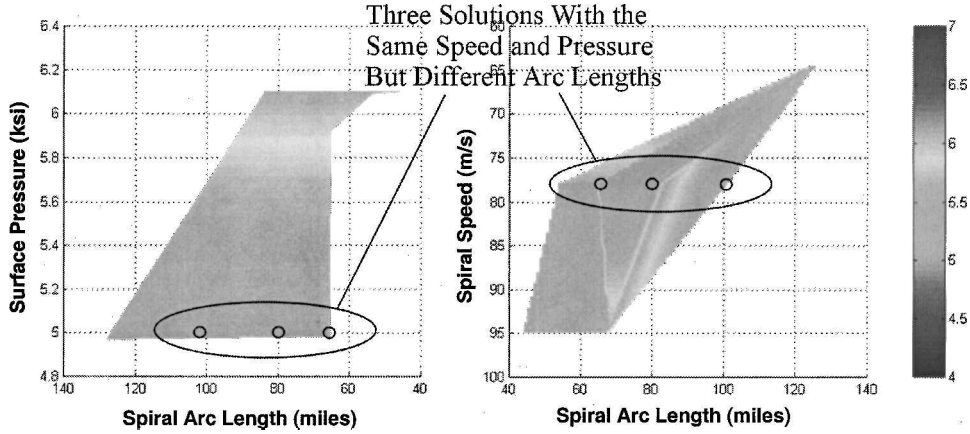

Fig. 12 Wall pressure vs spiral speed vs spiral track length for three of the successful launch solutions of Eq. (6) for the conditions of Eq. (10).

can be altered, and by how much, to compensate for a change in friction, but in the expectation that reasonable adjustments to any or all of the parameters can be made to counter the effects of a change in friction should future tests indicate an adjustment to Eq. (8) (for velocities above 2 km/s) is in order.

In summary, of the 243 parameter sets specified in Eq. (10), only 90 yielded a solution that produced a projectile speed of 8 km/s (or more). Of these 90, there was a subset of 10 that yielded notably different values for the track length and wall pressure (for each of these 10, there were 9 variations in θ_0 or R_0 that only slightly perturbed the length and pressure profiles). Among the 10 most distinct solutions, some were found to be more favorable than others from an engineering/construction vantage point. For example, Fig. 12 shows 3 of the 10 solutions that have the same frame speed ($r \times \dot{\psi}$), 78 m/s, and wall pressure, 5 ksi (at the time the projectile reaches 8 km/s), but with extremely different track lengths of 66, 80, and 102 miles, respectively. Although these three designs accomplish the same effect (namely, launching the projectile at 8 km/s), the difference in their costs (one being 40% shorter than the other) would be tremendous, proving the potential benefit of this type of parametric analysis.

The speed of the spiral frame is considered an important parameter because the higher the structural speed the higher the loads on moving parts (e.g., bearings) and the more wear and maintenance that can be expected. The most desirable solution is the one that has a low track speed, low wall pressure, and short track length. Although the relatively small range of parameters specified in Eq. (10) was useful in illustrating which parameters were most influential and it served to show how some solutions were more practical than others, it might yet be the case that an even better (easier to produce and maintain) design solution exists outside of the small parameter range examined thus far.

To explore the widest possible range of solutions with the minimum computer time and resources, it is sensible to distribute the collection of parameters in accordance with their degree of influence on the solution. As indicated, variation in θ_0 and R_0 does not produce significantly different results. Therefore, it makes sense to narrow the range of these two parameters and widen the range for the remaining three, namely, the gyration speed parameter $\dot{\psi}$, the gyration radius r, and the parameter governing the tightness of the spiral a. Accordingly, the 18,375 parameter sets of Eq. (12) were examined and found to yield a range of solutions that liberally bounds the region of practical interest:

$$\dot{\psi} = (\pi/2)(2n_1 - 1)\ \text{rad/s}, \quad \text{for} \quad n_1 = 1{:}35, \qquad R_0 = r + 4\ \text{m}$$

$$r = n_2 - 0.5\ \text{m}, \quad \text{for} \quad n_2 = 1{:}35, \qquad \dot{\phi}_0 = \dot{\psi}$$

$$a = (n_3 - 0.5) \times 0.05 \times r\ \text{m}, \quad \text{for} \quad n_3 = 1{:}15, \qquad \theta_0 = \pi/40\ \text{rad} \tag{12}$$

Out of the 18,375 different combinations of parameters in Eq. (12), there were 16,178 successful solutions that yielded a projectile speed of at least 8 km/s. Clearly, however, a structural speed

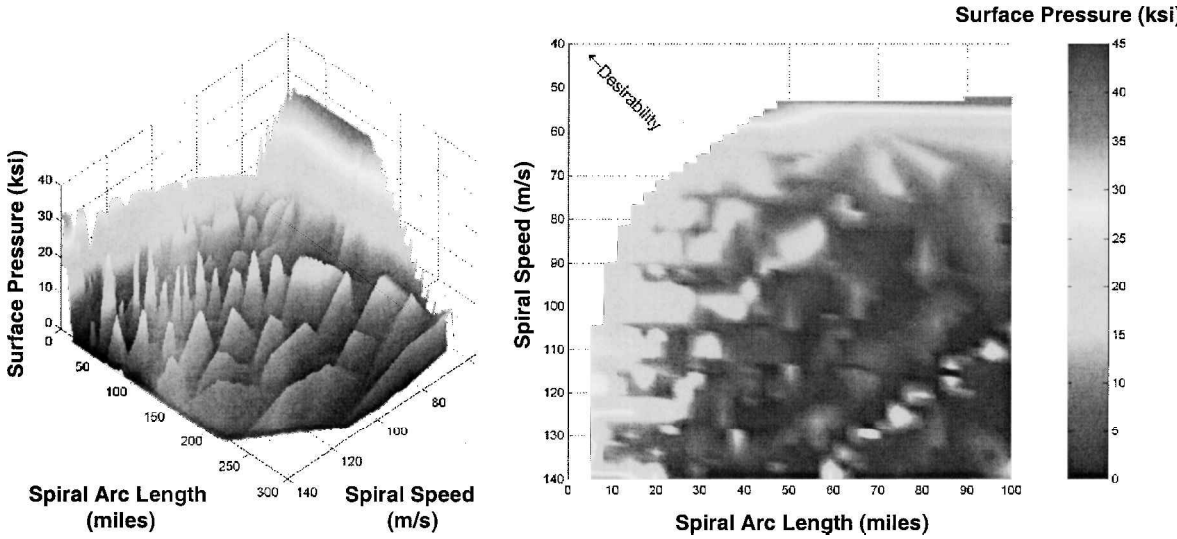

Fig. 13 Wall pressure vs spiral speed vs spiral track length, based upon Eqs. (6) and (12).

Table 1 Examples of the "most practical/optimum" slingatron track designs

Option	Structural speed, m/s	Wall pressure, ksi	Track length, miles	Weight, tons
A	139	**2**[a]	54	**2,700**
B	**53**	37	48	107,000
C	72	7	50	12,200
D	75	11	**28**	10,500

[a]Boldface indicates minimum values.

that is greater than the speed of sound (~335 m/s) is impractical; neglecting such high-speed cases would eliminate the majority of these solutions. A more reasonable frame speed might be several hundred meters per second slower. Searching the solution set, a subset of 600 solutions is found where the structural speed of the track is <140 m/s, and the track length is <~100 miles (Fig. 13).

At the upper speed end in this subset is a solution ($n_1 = 2, n_2 = 30, n_3 = 13$) where the structure is moving at 139 m/s (313 mph), the peak wall pressure is below 2 ksi, and the track length is a relatively moderate 54 miles. Based on the same approach used to determine the 8,500-ton track weight in the preceding (95-m/s, 6-ksi, 43-miles) example, this upper-speed-limit 54-mile track would weigh a relatively low 2,700 tons.

At the low-speed end a solution exists ($n_1 = 34, n_2 = 1, n_3 = 2$), where the track motion is slowed down to 53 m/s; the track length remains in the middle ground at 48 miles, but the wall pressure peaks at 37 ksi. The estimated weight of this lower-speed-limit track is 107,000 tons.

A more all around moderate solution ($n_1 = 7, n_2 = 4, n_3 = 6$) would have the track moving at 72 m/s with a wall pressure of 7 ksi and a track length, again in the midrange, of 50 miles. The estimated weight of this track would be 12,200 tons.

Perhaps the best solution compromise for structural speed, peak wall pressure, length, and weight is one ($n_1 = 10, n_2 = 3, n_3 = 7$) that produces midrange values for the frame speed at 75 m/s (170 mph), wall pressure at 11 ksi, weight at 10,500 tons, and low-end track length of 28 miles. (For reference, this slingatron would be the weight-motion equivalent of two fully loaded medium-sized river barges, each circling at ~5 Hz around an ~8-ft radius.)

Table 1 summarizes the four solutions just described, and Fig. 14 provides illustrations of other weight-equivalent structures on par with these track designs. Because the most practical of these solutions was well within the upper and lower limit boundaries on n_1, n_2, and n_3 [in Eq. (12)], it would appear that the parameter range was broad enough to capture the majority, if not all, of the optimum slingatron designs.

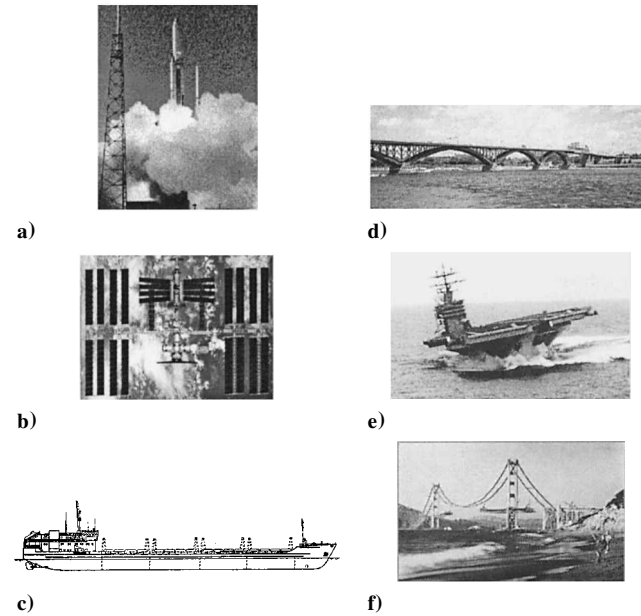

Fig. 14 Weight-equivalent structures on par with the track designs of Table 1: a) Titan IV Rocket: 340–380 tons, b) International Space Station: 520 tons, c) 500-ft fully loaded cargo ship: 8,000 tons, d) Large Steel River Bridge: 10,000 tons, e) 1000-ft fully loaded aircraft carrier: 80,000–100,000 tons, and f) Golden Gate Bridge: 200,000 tons.

Conclusions

This paper provides a physical explanation of the mechanism by which the mechanical device, referred to as a slingatron, akin to a hula hoop, can be used to launch a projectile into space. Furthermore, using MATLAB and Simulink the nonlinear differential equation of motion for a spiral slingatron was solved for a large range of input parameters. These solutions were sorted based upon whether or not the track configuration and gyration speed could accelerate a 1000-kg, 0.64-m-diam projectile to at least 8 km/s (assumed to be a sufficient speed to place such a payload into space). Finally, the most physically reasonably of these successful solutions were down selected. For example, a spiral track 28 miles long, weighting 10,500 tons, and having a structural speed of ~170 mph could be used to launch such a projectile into space.

With the type of information provided in this study (namely, structural speed, wall pressure, and track length), a more detailed track-design analysis could begin, leading to, among other things,

a total-dollar (or per-payload-pound) cost estimate for a slingatron-based Earth-to-space launch system.

References

[1]Tidman, D. A., Burton, R. L., Jenkins, D. S., and Witherspoon, F. D., "Sling Launch of Materials into Space," *Proceedings of 12th SSI/Princeton Conference on Space Manufacturing*, edited by B. Faughnan, Space Studies Inst., Princeton, NJ, 1995, pp. 59–70.

[2]Tidman, D. A., "Sling Launch of a Mass Using Superconducting Levitation," *IEEE Transactions on Magnetics*, Vol. 32, No. 1, 1996, pp. 240–247.

[3]Tidman, D. A., "Slingatron Mass Launchers," *Journal of Propulsion and Power*, Vol. 14, No. 4, 1998, pp. 537–544.

[4]Tidman, D. A., and Greig, J. R., "Slingatron Engineering and Early Experiments," *Proceedings of the 14th SSI/Princeton Conference on Space Manufacturing*, edited by B. Faughnan, Space Studies Inst., Princeton, NJ, 1999, pp. 306–312.

[5]Liepman, H. W., and Roshko, A., *Elements of Gasdynamics*, Wiley, New York, 1957, p. 64.

[6]Tidman, D. A., "Slingatron: a High Velocity Rapid Fire Sling," *Proceedings of the 10th U.S. Army Gun Dynamics Symposium*, edited by Mehmet Erengil, Inst. for Advanced Technology, Austin, TX, Dec. 2001, pp. 661–678.

[7]Dorf, R. C., *The Engineering Handbook*, CRC Press, Boca Raton, FL, 1996, p. 85.